

# About nonlinear behavior of unidirectional plant fiber composite

Christophe Poilâne, Florian Gehring, Haomiao Yang and Fabrice Richard

**Abstract** At room condition and standard speed, unidirectional glass fiber reinforced organic polymers show linear behavior under longitudinal loading (the same with carbon fiber). Oppositely, plant-based reinforced organic polymers often show nonlinear behavior. We describe a viscoelastoplastic model – based on eight independent parameters – dedicated to simulation of plant fiber composite mechanical behavior, previously validated with flax twisted yarn/epoxy composite at room condition. We analyse now an unidirectional flax/epoxy composite at different tensile speeds to promote a 'three apparent regions' mechanical behaviour visible in case of longitudinal loading. We show that adding of strengthening parameter is a good solution to improve mechanical behaviour model of plant fibre composite.

## 1 Introduction

Imagine a baseball bat mainly made of long plant fibre composite. Imagine this baseball bat – initially straight – which become more and more curved as we use it, even in case of normal use. Because it will be more and more difficult to play with, we can say that this baseball bat has been badly designed! It could be the case when designers ignore the fact that the constitutive composite material is not only elastic. . .

---

Christophe Poilâne  
Normandie Université, Esplanade de la Paix, 14032 Caen, e-mail: christophe.poilane@unicaen.fr

Florian Gehring  
Normandie Université, Esplanade de la Paix, 14032 Caen, e-mail: florian.gehring@unicaen.fr

Haomiao Yang  
Normandie Université, Esplanade de la Paix, 14032 Caen, e-mail: haomiao.yang@unicaen.fr

Fabrice Richard  
Université Bourgogne Franche Comté, 32 Av. de l'observatoire 25000 Besançon, e-mail: fabrice.richard@univ-fcomte.fr

Indeed, plant-based reinforced polymer often presents nonlinear mechanical behaviour at normal condition. This becomes particularly evident for tensile loading in fibre direction, with the presence of a yield point which separates tensile curve in two regions. For convenience we name the first region 'elastic', the second region being none elastic [1]. This is the case for flax fibre reinforcement [1, 2, 3, 4]. This is visible on experimental curves in articles that do not deal only with unidirectional reinforcement [2, 5], but also with reinforcement by random mat of flax [5, 6, 7]. This is finally the case for other (than flax) plant fibre composite [5, 8]. The yield point occurs at a very low level of strain, between 0.1 % to 0.3 % according to experimental conditions and measurement methods [3, 9]. Some authors develop models in order to simulate this particular mechanical behaviour [10, 11, 8, 12]; this will give the possibility to engineers to improve design of plant fibre composite parts. Such approach is very important, because the nonlinear behaviour is one of the differences between common fibre composite and plant fibre composites.

In a previous work [1] we proposed a viscoelastoplastic model to study the nonlinear effects of plant fibre composite. The used material was made by epoxy resin and twisted yarn of flax, as reinforcement. We assume that this reinforcement is quasi-unidirectional (quasi-UD). We identified eight parameters to correctly simulate the mechanical behaviour of flax/epoxy quasi-UD. Fitting and parameters identification were done by repetitive progressive loading (RPL) and creep test in the elastic region, at normal condition (room temperature, usual speed, normal humidity). Validation was done by creep test and relaxation test, both in the non elastic region. The used parameters take into account viscoelastic and viscoplastic contributions. The model do not necessitated of reorientation parameter, but we observed a contraction of the elastic region during loading. The first region of tensile curves is quasi-elastic and the second region is viscoelastoplastic.

## 2 Phenomenological model

The aim of constitutive phenomenological model is to provide an accurate prediction of uniaxial mechanical response of flax fibre reinforced polymer (FFRP). We particularly try to simulate the two regions' mechanical behaviour of FFRP described in introduction. A viscoelastoplastic model about FFRP behaviour has been previously developed [13]. The parameters of this model have been identified on 'UD' and 'quasi-UD' reinforcements based on twisted yarn [1]. UD are constituted by 'big' (more than 100 tex) non-woven yarns aligned in one direction only. Quasi-UD are constituted by small (minor to 50 tex) woven yarns, woven in two perpendicular directions: warp and weft. The weft yarns – which are ten times fewer in number than warp yarns – are needed for the ply handiness.

The total strain is partitioned in an elastic part (instantaneous reversible strain) and an inelastic part which is the sum of viscoelastic contribution (time-dependent reversible strain) and viscoplastic contribution (time-dependent irreversible strain):

$$\boldsymbol{\varepsilon} = \boldsymbol{\varepsilon}^e + \boldsymbol{\varepsilon}^{in} = \boldsymbol{\varepsilon}^e + \boldsymbol{\varepsilon}^{ve} + \boldsymbol{\varepsilon}^{vp}. \quad (1)$$

In the context of thermodynamics, physical phenomena can be described with a precision which depends on the choice of the nature and the number of state variables. The state variables, also called thermodynamic or independent variables, are the observable variables and the internal variables. The standardized framework [14] assumes that mechanical behaviour is obtained when two potentials are defined: a free energy density to define state laws and a dissipation potential to determine flow direction. Based on experimental results of ultimate stress, ultimate strain and Young modulus, and that elasticity and inelastic behaviours are uncoupled, the two potentials are proposed. The state laws can then be written as:

$$\boldsymbol{\sigma} = \rho \frac{\partial \psi}{\partial \boldsymbol{\varepsilon}^e} \quad (2)$$

$$X_i = \rho \frac{\partial \psi}{\partial \alpha_i} \quad (3)$$

where  $\alpha_i$  and  $X_i$  variables represent inelastic phenomena,  $\rho$  is the mass density, and  $\boldsymbol{\sigma}$  is the Cauchy's stress.

The evolution of internal variables is expressed as:

$$\dot{\boldsymbol{\varepsilon}}^{in} = \frac{\partial \Omega}{\partial \boldsymbol{\sigma}} = \dot{\boldsymbol{\varepsilon}}^{ve} + \dot{\boldsymbol{\varepsilon}}^{vp} \quad (4)$$

$$\dot{\alpha}_i = -\frac{\partial \Omega}{\partial X_i}. \quad (5)$$

The system of ordinary differential equations has been solved with an homemade simulation software, MIC2M [13], using an algorithm based on the Runge-Kutta method. An inverse approach is used to extract the parameters from the experimental strain measurements. This approach consists of an optimization problem where the objective is to minimize the gap between the experimental strain and the numerical results. The minimization problem was solved using an algorithm based on the Levenberg-Marquardt method coupled with genetic approach implemented in MIC2M software [13]. To determine if the information is suitable for reliable parameter estimation, a practical identifiability analysis was performed on results [1]. This identifiability analysis is based on local sensitivity functions. Such functions quantify the relationship between the outputs and the parameters of the model. Poor identifiability of the model parameters can be due to a small sensitivity of the model results to a parameter, or by a linear approximation dependence of sensitivity functions on the results with respect to the parameters (see [1] for detail). This approach led our team to model the mechanical behaviour of the FFRP by a phenomenological model with kinematic hardening taking viscosity into account. The viscoelastoplastic model was identified in the case of uniaxial test of unidirectional twisted yarn/epoxy composite [1]. The particularity of the reinforcement is the misorientation of constitutive fibres due to the use of twisted yarns. Based

on experimental results, the free energy and dissipation potential are proposed in following equations:

$$\Psi(\varepsilon^e, \alpha_i) = \frac{1}{2\rho} E(\varepsilon^e)^2 + \frac{1}{2\rho} \sum_{i=1}^3 C_i \alpha_i^2 \quad (6)$$

$$\Omega = \Omega^{ve} + \Omega^{vp} = \frac{1}{2\eta} (\sigma - X_1)^2 + \frac{1}{2K} \langle f \rangle^2 \quad (7)$$

with

$$f = |\sigma - X_2 - X_3| - \sigma_Y + \frac{\gamma_3}{2C_3} X_3^2 \quad (8)$$

where  $\rho$  is the mass density,  $E$  and  $\sigma_Y$  are the Young's modulus and the initial yield stress respectively,  $\eta$  and  $K$  are viscosity coefficients corresponding to elastic and plastic phenomena, respectively.  $C_1$  is the viscoelastic stiffness.  $C_2$ ,  $C_3$  and  $\gamma_3$  are hardening coefficients.  $C_2$  characterizes linear kinematic hardening.  $C_3$  and  $\gamma_3$  refer to nonlinear kinematic hardening coupled to a contraction of elastic region in order to improve the unloading modelling in RPL tests. The state laws for mechanical behaviour becomes:

$$\sigma = E\varepsilon^e \quad (9)$$

$$X_i = C_i \alpha_i. \quad (10)$$

and the evolution of internal variables defined becomes:

$$\dot{\varepsilon}^{ve} + \dot{\varepsilon}^{vp} = \frac{1}{\eta} (\sigma - X_1) + \frac{\langle f \rangle}{K} \text{sign}(\sigma - X_2 - X_3) \quad (11)$$

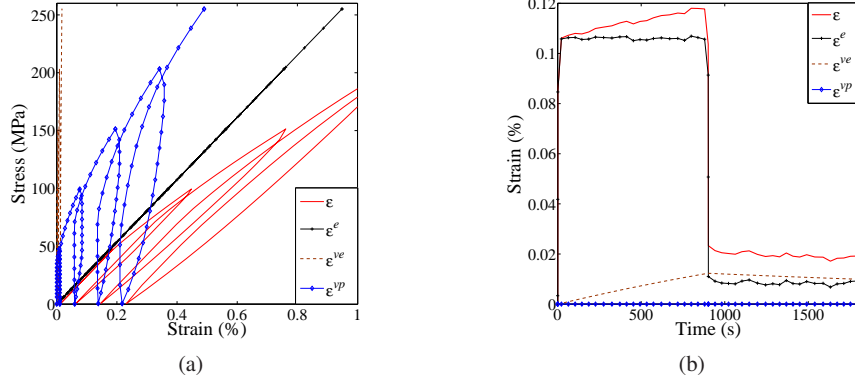


**Fig. 1** Simulation response according to elastic contribution, viscoelastic contribution and viscoplastic contribution for (a) RPL test, and (b) creep test at 29 MPa; the tests were conducted on unidirectional twisted yarn/epoxy composite at room condition and standard speed.

$$\dot{\alpha}_1 = \frac{1}{\eta}(\sigma - X_1) \quad (12)$$

$$\dot{\alpha}_2 = \frac{\langle f \rangle}{K} \text{sign}(\sigma - X_2 - X_3) \quad (13)$$

$$\dot{\alpha}_3 = \frac{\langle f \rangle}{K} \left[ \text{sign}(\sigma - X_2 - X_3) - \frac{\gamma_3}{C_3} X_3 \right]. \quad (14)$$

From a rheological point of view the model proposed in [1] is, for elastic contribution, a linear spring  $E$ , and for viscoelastic contribution, a classical Kelvin-Voigt model which comprises a linear viscous damper and a linear spring connected in parallel. For viscoplastic contribution, a more complex model is required; it consists in adding two kinematic hardenings: a linear kinematic hardening and a nonlinear kinematic hardening. In addition, a coupling between translation and contraction of the elastic region during loading is added. Finally, seven inelastic parameters have to be identified: viscosity coefficient in elastic region  $\eta$ , viscoelastic stiffness  $C_1$ , initial yield stress  $\sigma_Y$ , viscosity coefficient in plastic region  $K$ , kinematic hardening coefficient  $C_2$ , nonlinear hardening  $C_3$ , and nonlinear hardening recall  $\gamma_3$ . The eighth parameter, namely the Young's modulus, was chosen from experimental measurement. The inverse method approach was used to extract constitutive inelastic parameters from the strain measurements from two tests: test A = repetitive progressive loading in tension, test B = creep in tension in 'elastic' region. The RPL is chosen to activate mainly viscoplastic phenomena and the creep test in 'elastic' region is chosen to activate mainly viscoelastic phenomena. Fig. 1(a) coming from [1] shows RPL simulation (left) and creep simulation (right). The used parameters have been identified from unidirectional twisted yarn/epoxy composite tests at room temperature and standard speed (strain rate  $10^{-6} \text{s}^{-1}$ ). The total strain (in red) is partitioned by three contributions (elastic in black, viscoelastic in dotted line, viscoplastic in

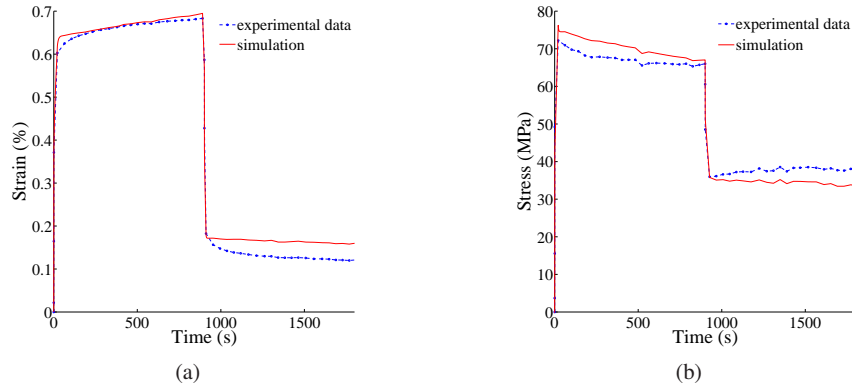


**Fig. 2** Experimental data and simulation for (a) creep test at 126 MPa, and (b) relaxation test at 0.33 %; the tests were conducted on unidirectional twisted yarn/epoxy composite at room condition and standard speed.

blue). Elastic contribution is naturally activated all over the test. Viscoelastic contribution is very low at room condition and standard speed; creep test mainly shows elastic contributions, as expected.

At room temperature, the proposed model allows us to correctly simulate the behaviour of flax yarn reinforced epoxy composite in repetitive progressive loading, creep test (Fig. 2(a)) and relaxation test (Fig. 2(a)). The value of the eight identified parameters is given in table 1.

In conclusion, for unidirectional twisted flax yarn/epoxy composite at room condition and standard speed, the first region of monotonic tensile curves is quasi-elastic and the second region is viscoelastoplastic.

**Table 1** Elastic and inelastic material parameters for UD twisted flax yarn/epoxy composite.

Parameter	Definition	Identified value
$E$ (MPa)	Young's modulus	$2.69 \times 10^4$
$\eta$ (MPa s)	viscosity coefficient in elastic region	$1.78 \times 10^8$
$C_1$ (MPa)	viscoelastic stiffness	$6.30 \times 10^4$
$\sigma_Y$ (MPa)	initial yield stress	$3.32 \times 10^1$
$K$ (MPa s)	viscosity coefficient in plastic region	$2.24 \times 10^5$
$C_2$ (MPa)	kinematic hardening coefficient	$3.39 \times 10^4$
$C_3$ (MPa)	nonlinear hardening	$6.85 \times 10^4$
$\gamma_3$	nonlinear hardening (recall)	$9.64 \times 10^2$

### 3 Discussion

The phenomenological model presented in previous section did not need a 'strengthening parameter' to correctly simulate standard flax fibre composite in normal condition. The idea of a strengthening parameter is due to one of the stronger assumption researchers make in case of bast fibre reinforced polymer: the possibility for microfibrils to reorientate themselves during longitudinal loading (microfibril being the main component of bast fibres), even when fibres are trapped inside the matrix. The re-orientation of microfibrils has been demonstrated experimentally on elementary fibre and bundle of fibres under tensile test [15]. It has been correlated to experimental tensile curve by an inverse approach using finite element model [16]. Then the question of this reorientation when bast fibres are used as reinforcement in composite is very logical. In case of reinforcement reorientation during longitudinal loading, whatever the scale of the reinforcement – untwist at the scale of microfibril, untwist at the scale of yarn, in-plane reorientation at the scale of ply – we assume that the Young's modulus of the material has to be increase. But such Young's modulus increase was not needed for simulating mechanic of viscoelastoplastic yarn reinforced epoxy composite [1].

**Fig. 3** Example of unidirectional ply of flax [18] (without matrix). Some of the fibres (elementary fibre or bundle of fibres) are not aligned in the longitudinal direction, but such misaligement is minor.



In order to test our model for more complex cases than previous one [1], the first need is to improve the direction of the fibres inside composite. Indeed, it is clear that twisted flax yarn as reinforcement is not the best candidate to activate the reorientation of microfibrils inside a composite. It is known that in case of twisted yarn some of the fibres are oriented in the main direction [17]. But globally fibre orientation follows a statistical distribution the with major part of fibres aligned not in the longitudinal direction. A totally unidirectional flax reinforced polymer is now possible to make with industrial product. Fig. 3 shows one industrial flax ply used to make such long fibre composite [18]. It is clearly visible that the fibres are mainly oriented in the longitudinal direction (the vertical one). In this product, there are no any weft yarn and no any sewing to link the fibres together. The process we use to make composite plates with flax and epoxy matrix is the hot platen press, as in [1]. The dry flax reinforcement was not treated before use, the objective of the analysis being not to obtain the highest properties but to analyse unidirectional flax composite mechanical behaviour. The reinforcement inside the final composite plate is constituted by a mix of elementary fibres and bundles of fibre (bundles as they are in flax stem). Consequently, this reinforcement is mainly oriented in

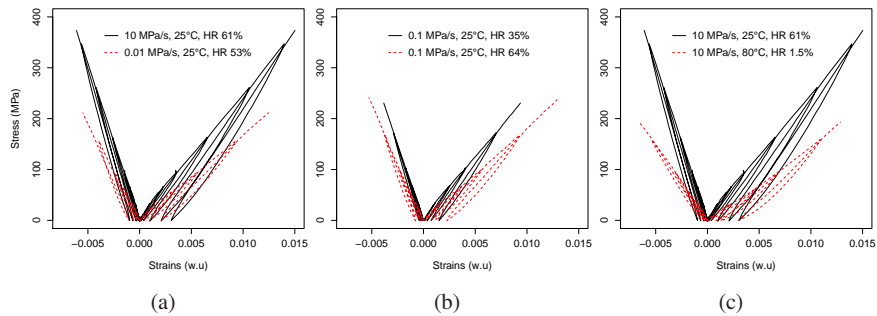


**Fig. 4** Effect of (a) speed (b) moisture only and (c) temperature/moisture, on RPL curves in longitudinal tensile of unidirectional flax composite.

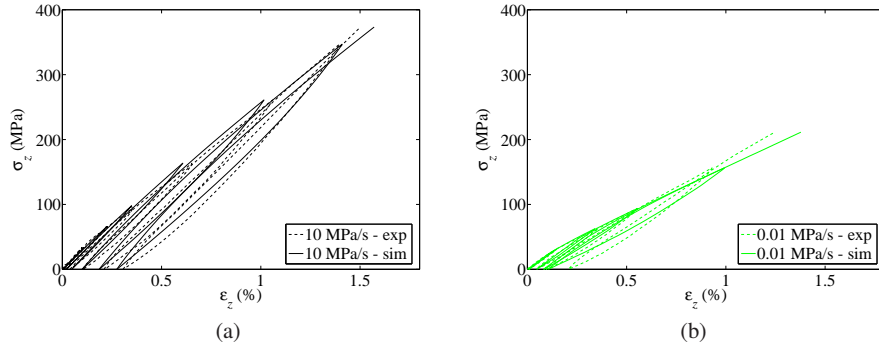


**Fig. 5** RPL experiment and simulation with the phenomenological model presented in section 2. The value of the eight parameters are given in table 2.

the longitudinal direction of composite, which is optimal organisation in term of mechanical behaviour analysis.

Once the orientation of reinforcement optimal, the increase of the specimen temperature is one possibility to make easiest the activation of viscous effects of flax composite (Fig. 4(c)) [1]. Firstly, the rigidity of epoxy matrix decreases with increasing temperature. Particularly, the mechanical properties of thermosetting media drastically decrease when temperature nears to the glass transition temperature  $T_g$  of the material. Secondly, high temperature activates viscoelastic properties of bast fibres [19]. One macroscopic consequence of temperature increase is to make possible a description of tensile curve by three apparent regions (see dotted line in Fig. 4(c)). Consequently, one simple idea for testing phenomenological model efficiency with unidirectional reinforcement is to increase the testing temperature. Note that when we do not set the relative humidity in oven during tensile test, the increase of temperature is correlated to a decrease of humidity, as shows in Fig. 4(c). Note also that the increase of specimen moisture itself promotes viscous effects of flax composite – as shows in Fig. 4(b) – and makes also visible a three region apparent tensile curve [4]. Which is a second way but not simple to test phenomenological model efficiency in non trivial case. Another way, more simple, is to decrease the strain rate of the tensile test. Indeed when the strain rate is low, viscous effects exposed in [1] are more visible (see Fig. 4(a)). In other terms, the mechanisms which are responsible of viscous effects are more easy to activate with 'low tensile speed', 'high testing temperature' or 'high specimen moisture'.

Eventually, to test our model with unidirectional flax composite we chose repetitive progressive loading at four different stress rates ( $0.01 \text{ MPa s}^{-1}$  to  $10 \text{ MPa s}^{-1}$ ). For the lower speed (Fig. 5(b)), experimental tensile curve seems to be constituted by three apparent regions instead of two, the first region being quasi-elastic, the third region showing increase of apparent tangent modulus. Let us add that the increase of apparent tangent modulus can be described by the viscous parameters of previous constitutive model.



**Table 2** Elastic and inelastic material parameters for unidirectional flax/epoxy composite

Parameter	Definition	Identified value
$E$ (MPa)	Young's modulus	$3.15 \times 10^4$
$\eta$ (MPa s)	viscosity coefficient in elastic region	$1.98 \times 10^6$
$C_1$ (MPa)	viscoelastic stiffness	$7.72 \times 10^4$
$\sigma_Y$ (MPa)	initial yield stress	$2.38 \times 10^1$
$K$ (MPa s)	viscosity coefficient in plastic region	$1.92 \times 10^7$
$C_2$ (MPa)	kinematic hardening coefficient	$3.92 \times 10^4$
$C_3$ (MPa)	nonlinear hardening	$4.26 \times 10^4$
$\gamma_3$	nonlinear hardening (recall)	$1.62 \times 10^3$

The previous phenomenological model was possible to fit on experimental data with the same set of inelastic parameters (but different values). Fig. 5 shows the best fits we obtained for both extremal speeds. The eight identified parameters are given in table 2. It is clearly visible that the simulation of the test at the lower tensile speed do not correlate very well with the experimental data (Fig. 5(b)). In that case, the increase of apparent tangent modulus – visible on fourth and fifth load – was not possible to simulate. Moreover, indepth look on Fig. 5(a) shows that this behavior was neither possible to simulate on seventh load of the test at  $10 \text{ MPa s}^{-1}$ . Something like a strengthening effect has not been taken into account with our model for a strain above 1 % (depending on strain rate). Consequently to this underestimation of apparent rigidity, the permanent strains predicted by our model of are lower than the experimental ones, loop after loop.

## 4 Conclusion

We just showed an apparent cycling strengthening in tensile winch is not possible to simulate with our previous viscoelastoplastic model. For adapted material and specific tests, the difference between experimental data and simulation – once the viscoelastoplastic parameters identified – is noticeable. Low speed repetitive progressive loading tests in tensile were used here, but we make the assumption that high temperature tests or tensile tests on moisturized specimens should be other good possibilities also. Finally, we propose as strong assumption that the add of strengthening parameter(s) to the initial model [1] offers a good solution to improve simulation. Fig. 6 shows the first result we obtain with the same data as used for Fig. 5 when we substitute nonlinear hardening  $C_3$  and  $\gamma_3$  with two strengthening parameters. The fitting of experimental data by simulation is clearly improved at the low tensile speed (Fig. 6(b)). Although this new approach is not totally validated at this day, it offers an elegant solution because it seems easy to correlate cycling strengthening to reinforcement reorientation by longitudinal loading in case of unidirectional flax composite. In a near future, analysis of such model will help

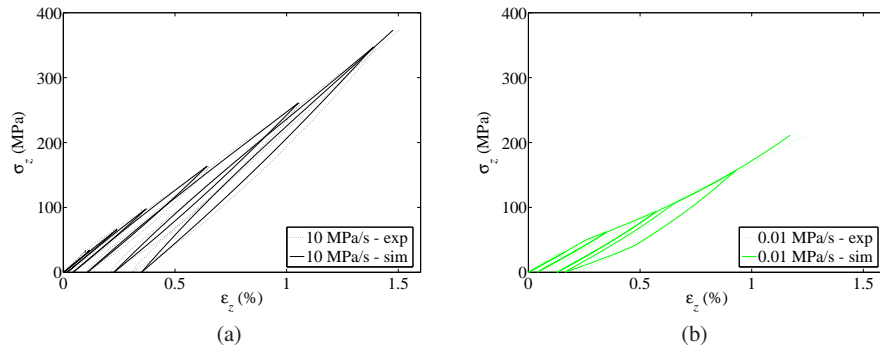


**Fig. 6** RPL experiment and new simulation with strengthening parameters.

at exploring the origin of the mechanical behavior of plant-based reinforced organic polymers.

**Acknowledgements** China Scholarship Council (CSC) is acknowledged for the financial support.

## References

1. C. Poilâne, Z.E. Cherif, F. Richard, A. Vivet, B. Ben Doudou, J. Chen, *Composite Structures* **112**, 100 (2014)
2. K. Oksman, *J Reinf Plast Comp* **20**, 621 (2001)
3. J.C. Hughes, J. Carpenter, C. Hill, *J Mat Sci* **42**, 2499 (2007)
4. D. Scida, M. Assarar, C. Poilâne, R. Ayad, *Compos Part B-Eng* **48**, 51 (2013)
5. G. Lebrun, *Composite Structures* **103**, 151 (2013)
6. Z.E. Cherif, C. Poilâne, L. Momayez, J. Chen, *Revue des Composites et des Matériaux avancés* **21**, 119 (2011). Comportement mécanique des renforts et des composites tissés, JST AMAC, Orléans, Mai 26-27, 2010
7. Z.E. Cherif, C. Poilâne, L. Momayez, J. Chen, *Matériaux & Techniques* **100**, 459 (2012). Matériaux 2010, Nantes, FRANCE, Oct 18-22, 2010
8. A. Rubio-López, T. Hoang, C. Santiuste, *Composite Structures* **155**, 8 (2016)
9. D.U. Shah, *Compos Part A-Appl S* **83**, 160 (2016)
10. J. Andersons, J. Modniks, E. Sparmins, *J Reinf Plast Comp* **34**(3), 248 (2015)
11. A. Chiali, W. Zouari, M. Assarar, H. Kebir, R. Ayad, *J Reinf Plast Comp* pp. 1–16 (2016)
12. J. Sliseris, L. Yan, B. Kasal, *Compos Part B-Eng* **89**, 143 (2016)
13. F. Richard. MIC2m, modélisation et identification du comportement mécanique non linéaire des matériaux (1999). URL <http://mic2m.univ-fcomte.fr>
14. B. Halphen, Q.S. Nguyen, *J de Mécanique* **14**, 39 (1975)
15. A. Bourmaud, C. Morvan, A. Bouali, V. Placet, P. Perré, C. Baley, *Ind Crop Prod* **44**, 343 (2013)
16. A. Del Mastro, F. Trivaudey, V. Guicheret-Retel, V. Placet, L. Boubakar, *J Mat Sci* (2017)
17. J. Baets, D. Plastria, J. Ivens, I. Verpoest, *J Reinf Plast Comp* **33**, 493 (2014)
18. Lineo - Flax Fiber Impregnation. URL <http://www.lineo.eu/>. [accessed 2016-01-24]
19. P. Placet, *Compos Part A-Appl S* **40**, 1111 (2009)